Bell, R. A., & Saunders, J. K. (1970) *J. Chem. Soc. D*, 1078.
Bender, M. L., Kezdy, F. J., & Gunter, C. R. (1964) *J. Am. Chem. Soc. 86*, 3714–3721.
Brooks, D. J., Busby, S. J., & Rada, G. R. (1974) *Eur. J. Biochem. 48*, 571–578.
Campbell, I. D., Dwek, R. A., Price, N. C., & Rada, G. K. (1972) *Eur. J. Biochem. 30*, 339–347.
Chang, Y. C., & Graves, D. J. (1985) *J. Biol. Chem. 260*, 2709–2714.
Chang, Y. C., McCalmont, T., & Graves, D. J. (1983) *Biochemistry 22*, 4987–4993.
Chang, Y. C., Scott, R. D., & Graves, D. J. (1986) *Biochemistry 25*, 1932–1939.
Gerig, J. T. (1978) *Biological Magnetic Resonance* (Berliner, L. T., & Reuben, J., Eds.) Vol. 1, pp 139–203, Plenum Press, New York and London.
Graves, D. J., & Wang, J. L. (1972) *Enzymes (3rd Ed.) 7*, 435–481.
Graves, D. J., Carlson, G. M., Skuster, J. R., Parrish, R. F., Carty, T. J., & Tessmer, G. W. (1975) *J. Biol. Chem. 250*, 2254–2258.
Helmreich, E., Michaelides, M. C., & Cori, C. F. (1967) *Biochemistry 6*, 3695–3710.
Hull, W. E., & Sykes, B. D. (1976) *Biochemistry 15*, 1535–1546.
Ikawa, M. (1968) *Biochem. Prep. 12*, 117–121.
Jencks, W. P. (1969) in *Catalysis in Chemistry Enzymology*, McGraw-Hill, New York and London.
Johnson, L. N., Jenkins, J. A., Stuart, D. I., Stura, E. A., Wilson, S., & Zanotti, G. (1980) *J. Mol. Biol. 140*, 565–580.
Kastenschmidt, L. L., Kastenschmidt, J., & Helmreich, E. (1968) *Biochemistry 7*, 3590–3608.
Klein, H. W., & Helmreich, E. J. M. (1980) *Angew. Chem., Int. Ed. Engl. 19*, 441–455.
Korytnyk, W., & Ikawa, M. (1970) *Methods Enzymol. 18*, 524–566.
Korytnyk, W., & Kravastava, S. C. (1973) *J. Med. Chem. 16*, 638–642.
Madsen, N. B., & Withers, S. G. (1984) *Coenzymes and Cofactors: Pyridoxal Phosphate and Derivatives* (Dolphin, D., Paulson, R., & Arramovic, O., Eds.) pp 1–29, Wiley, New York.
Madsen, N. B., Kavinsky, P. J., & Fletterick, R. J. (1978) *J. Biol. Chem. 253*, 9097–9101.
McLaughlin, P. J., Stuart, D. I., Klein, H. W., Oikonomakos, N. G., & Johnson, L. N. (1984) *Biochemistry 23*, 5862–5873.
Parrish, R. F., Uhing, R. J., & Graves, D. J. (1977) *Biochemistry 16*, 4824–4831.
Sansom, M. S. P., Babu, Y. S., Hajdu, J., Stuart, D. I., Stura, E. A., & Johnson, L. N. (1984) *Chemical and Biological Aspects of Vitamin B_6 Catalysis, Part A* (Evangelopoulos, A. E., Ed.) pp 127–146, Alan R. Liss, Inc., New York.
Sprang, S. R., & Fletterick, R. J. (1979) *J. Mol. Biol. 131*, 523–551.
Sprang, S. R., Goldsmith, E. J., Fletterick, R. J., Withers, S. G., & Madsen, N. B. (1982) *Biochemistry 21*, 5364–5371.
Thomas, J. A., Schlender, K. K., & Larner, J. (1968) *Anal. Biochem. 25*, 486–499.
Withers, S. G., Madsen, N. B., Sprang, S. R., & Fletterick, R. J. (1982) *Biochemistry 21*, 5372–5382.

DNA Structure Equilibria in the Human c-*myc* Gene†

T. C. Boles and Michael E. Hogan*
Department of Molecular Biology, Princeton University, Princeton, New Jersey 08544
Received April 28, 1986; Revised Manuscript Received September 5, 1986

ABSTRACT: We have employed analytical S1 nuclease analysis to identify sites with altered DNA secondary structure in the human c-*myc* gene. We have mapped several sites of that kind in vitro at one-base resolution but have focused our attention on one particularly stable conformational isomer which occurs approximately 270 base pairs upstream from the preferred transcription origin. We have analyzed the kinetics of that conformational equilibrium as a function of supercoil density and enzyme concentration and find that DNA structure in this region is adequately modeled as a two-state equilibrium between an undistorted (S1 nuclease insensitive) and a distorted (S1-sensitive) state. We find that at fixed supercoil density, S1 nuclease cleavage at this DNA segment can be altered in vitro by a DNA sequence change as far away as 1500 bases. We also find that the S1 nuclease cleavage at this site can be dramatically enhanced by the binding of small RNA molecules. On the basis of an analysis of S1 cutting kinetics and an analysis of DNA sequence at the S1 cleavage site, we conclude that RNA may bind directly to DNA, thereby shifting the underlying conformational equilibrium. Together, these data suggest that as a class, short RNA molecules could serve as site-specific regulatory elements in the *myc* gene and elsewhere.

Recently, on the basis of the use of chemical and enzymatic probes, sites have been identified in cloned genes which appear to have assumed an atypical DNA secondary structure. Sites of that kind have been identified in the chicken β^A-globin gene (Schon et al., 1983; Nickol & Felsenfeld, 1983; Wang & Hogan, 1985), in the *Drosophila* HPS70 gene (Mace et al., 1983), in the sea urchin histone gene cluster (Hentschel, 1982), and in a variety of synthetic DNA inserts (Pullyblank et al., 1985; Kohwi-Shigematsu & Kohwi, 1985).

Several laboratories are attempting to rationalize those data in structural terms, and some generalizations have been made.

† This work was supported by Grant RO1 CA39527-01 from the National Cancer Institute.

0006-2960/87/0426-0367$01.50/0

On the basis of chemical and S1 nuclease analysis, it has been proposed that segments with 2-fold symmetry can assume cruciform (stem–loop) structures in highly supercoiled plasmid molecules (Lilley, 1980). When alternating purine–pyrimidine segments are included into supercoiled plasmids, they appear to undergo a right-hand B- to left-hand Z-helix transition (Klysik et al., 1981). In supercoiled plasmids, long synthetic polypurine–polypyrimidine segments appear to assume an altered conformation which has been postulated to be a loop (Nickol & Felsenfeld, 1983) or perhaps a left-hand helix form (Cantor et al., 1984).

The biological significance of such secondary structure variation is unclear. Nuclease and chemically sensitive sites in genes are often nearby regions which have been identified as having functional significance. However, structure/function relationships of that kind are controversial (Sinden et al., 1983). It is interesting to consider the possibility that structurally altered DNA segments might serve as a regulatory signal for a specific ligand binding event, but a clear-cut example of such a relation is not now available.

In previous work involving altered DNA conformation in the adult β-globin gene, we concluded that (as might be expected intuitively) the phenomenon of rare nuclease sensitivity in genes must be considered in equilibrium terms; i.e., sites become especially sensitive to a probe such as S1 nuclease because they possess the capacity to equilibrate between an ordinary helix structure and one which is recognized by the enzyme (Wang & Hogan, 1985).

Here we apply such equilibrium concepts to the study of DNA conformational equilibria in the human c-*myc* gene. We have chosen to study this cloned gene fragment in structural and kinetic terms because a preliminary computer analysis suggested to us that the *myc* gene possesses regions with a sequence which might be capable of forming an atypical DNA secondary structure. Moreover, the c-*myc* gene is notable in that control of its expression may be linked to the position of the gene within chromosomes; i.e., activation of c-*myc* to an oncogenic state is sometimes accompanied by rearrangement events which alter the identity of nearby DNA segments but which leave coding and intron sequences intact (Leder et al., 1983). That activation has been explained as due to the effect of distant enhancers or distant repressive elements, acting in cis upon the c-*myc* gene. Therefore, our second reason for studying c-*myc* structure is to determine if such long-range sequence effects can be detected in vitro, in terms of their effects on DNA secondary structure within the gene.

Materials and Methods

Plasmids. The human genomic c-*myc* (plasmid pHM3) was obtained from the laboratory of Michael Cole. It contains an 8 kilobase (kb) *Eco*RI–*Hin*dIII fragment of human genomic DNA cloned into the corresponding restriction sites of pBR322 (Bolivar et al., 1977). The insert contains the entire c-*myc* gene with approximately 2 kb of sequence to the 5′ side and 0.6 kb to the 3′ side of its coding sequences (see Figure 6B for a map). This plasmid was grown in *E. coli* strain DH1.

The plasmid pM-HX was constructed by ligating the 3.5 kb *Hin*dIII–*Xba*I fragment from pHM3 into pUC12 (Viera & Messing, 1982). This fragment contains the first (nontranslated) exon of the c-*myc* gene and 2 kb of 5′-flanking sequence (Figure 1C). In the experiments shown in Figures 1 and 2, the plasmid was grown in *Escherichia coli* strain JM103 (Messing, 1983). All other experiments use plasmid grown in HB101.

Plasmid-containing bacteria were shaken overnight at 37 °C in LB medium (Maniatis et al., 1982) supplemented with 50 μg/mL ampicillin. Plasmids were prepared by a standard alkaline extraction procedure and CsCl–ethidium bromide density gradient centrifugation as described (Maniatis et al., 1982). The gradient fraction containing supercoiled plasmid was repeatedly extracted with butanol and then dialyzed extensively against TE buffer [10 mM tris(hydroxymethyl)-aminomethane hydrochloride (Tris-HCl), pH 8.0, and 1 mM ethylenediaminetetraacetic acid (EDTA)]. Unless otherwise specified in the figure legends, all plasmid preparations were further purified by Sepharose 6B chromatography (column size 2.5 cm × 35 cm, TE buffer + 50 mM NaCl, 4 °C) to remove low molecular weight, UV-absorbing species which are present following the gradient step. The elution profile was monitored by UV absorbance. The purified plasmid elutes in the excluded volume while the low molecular weight material elutes as a broad symmetric peak in the included volume. We routinely loaded samples of up to 2 mg of CsCl-purified plasmid in a volume of 2 mL. Under these conditions, the column resolves the two peaks completely.

Alteration of Plasmid Superhelical Density in Vitro. Throughout this paper, we will refer to plasmid superhelical density as previously defined (Bauer & Vinograd, 1968): $\sigma = \alpha - \alpha^0)/\alpha^0$ where α^0 = the size of the plasmid in base pairs/10.5.

In the experiments shown in Figures 1 and 2, highly supercoiled plasmids were prepared by a method employing DNase I and T4 ligase. Briefly, singly nicked plasmids were prepared by DNase I digestion in the presence of saturating ethidium bromide (100 μg/mL DNA, 1 μg/mL DNase I, 300 μg/mL ethidium, 10 mM Tris-HCl, pH 8.0, and 10 mM $MgCl_2$), digestion for 30 min at 25 °C. After purification by phenol–chloroform extraction and ethanol precipitation, the material was resuspended in ligase buffer (50 mM Tris-HCl, pH 8.0, 8 mM $MgCl_2$, 10 mM dithiothreitol, and 1 mM ATP) at a DNA concentration of 100 μg/mL. Ethidium bromide was added to 4.25×10^{-5} M, and the samples were equilibrated at 25 °C for several minutes. T4 DNA ligase (Boehringer) was added to 50 units/mL, and the mixture was incubated at 25 °C for 2 h. The plasmid was recovered by phenol extraction and ethanol precipitation.

In other experiments, samples of defined superhelical density were prepared by relaxing plasmids with eukaryotic topoisomerase I (topo I) (BRL) in the presence of varying amounts of ethidium bromide. The equilibrium binding constant for ethidium in these reactions were calculated from fluorescence titrations (LePecq & Paoletti, 1976) in topo I reaction buffer (10 mM Tris-HCl, pH 7.6, 50 mM KCl, 10 mM $MgCl_2$, 120 μg/mL DNA, and 133 units/mL topo I) and were found to be approximately 1×10^4 M^{-1}. For an individual topo I reaction, supercoil density was calculated by using that ethidium binding constant and the known dye and DNA concentrations and by assuming that ethidium untwists DNA by 26 °C per bound molecule.

S1 Digestion. S1 nuclease was obtained from Boehringer or Sigma. Allowing for differences in the definition of unit activity (1 Sigma unit = 30 Boehringer units), the two enzyme preparations behaved identically in our hands. In this paper, enzyme activities will be reported according to the Boehringer definition.

The buffer conditions for S1 digestion were 30 mM sodium acetate, pH 4.5, 150 mM NaCl, and 5 mM $ZnCl_2$. Typically, enough DNA for several time points was dissolved in S1 buffer at 50–100 μg/mL and equilibrated for 15 min at 37 °C. After removal of a zero time point, S1 nuclease was added to 500–1000 S1 units/μg of DNA. Time points containing equal

amounts of DNA (usually 4 μg) were removed. To terminate digestion, samples were diluted 2-fold with 150 mM Tris-HCl, pH 8.0, and then immediately extracted with an equal volume of phenol–chloroform. DNA was recovered by ethanol precipitation.

Purification of Low Molecular Weight Factors from Plasmid DNA. Plasmid pHM3 which had been purified by CsCl–ethidium bromide density gradient centrifugation was deproteinized by phenol–chloroform extraction and then subjected to Sepharose 6B chromatography. The elution profile was followed by UV absorbance. The fractions comprising the entire included volume were pooled, and sodium acetate (pH 5.2) was added to 0.3 M. The mixture was ethanol precipitated, rinsed with ethanol, dried in vacuo, and then resuspended in TE buffer (10 mM Tris-HCl and 1 mM EDTA, pH 7.6). These low molecular weight (LMW) factors were stored at −20 °C.

RNase T1 Digestion of Low Molecular Weight Factors. Low molecular weight factors obtained from Sepharose 6B chromatography of pHM3 were resuspended in TE buffer at an OD_{260} of 8. A 50-μL aliquot of this solution was digested with 7.5 units of RNase T1 (Boehringer) for 30 min at 37 °C. A control aliquot was incubated at 37 °C without addition of RNase. The samples were extracted 2 times with phenol to remove protein and then ethanol precipitated. The factors were resuspended in 5 μL of TE buffer, mixed with 4-μg aliquots of Sepharose 6B purified pHM3 in 50 μL of S1 buffer, and incubated for 30 min at 37 °C. The mixtures were then digested with 2000 units of S1 for 20 min at 37 °C as described above.

Kinetic Analysis of Site-Specific S1 Nuclease Cutting. Complementary antiparallel DNA strands are capable of forming a B-type Watson–Crick duplex, a structure which is not a good substrate for S1 nuclease. Therefore, those rare complementary DNA segments which do assume an S1-sensitive conformation must also be capable of existing as an enzyme-insensitive structure, if only transiently.

Here, we model such an equilibrium by a two-state formalism. We describe DNA at an interesting site as existing in either an S1-insensitive conformation (B) or an S1-sensitive conformation (A). In the context of this formalism, the addition of enzyme (E) and the subsequent production of site-specific cuts (P) can be described in terms of the equations:

$$\begin{aligned} &B \underset{k_{-1}}{\overset{k_1}{\rightleftharpoons}} A && \text{isomerization} \\ &A + E \underset{k_{-2}}{\overset{k_2}{\rightleftharpoons}} D && \text{enzyme binding} \\ &D \xrightarrow{k_3} P && \text{cutting} \end{aligned} \qquad (1)$$

Here, k_1 and k_{-1} refer to the apparent rate constants for formation and dissipation of the S1-sensitive conformation, k_2 is the bimolecular rate constant for S1 binding to A, and k_3 is a rate constant which describes the enzymatic strand-break reaction at A. In this simplified scheme, we have presumed that (as seen experimentally) S1 cutting of an ordinary duplex conformation is too slow to be significant.

In our enzyme cutting experiments, S1 (at a total concentration E_0) is mixed with DNA (at total concentration C_T), and then the time dependence of S1 cutting at A is monitored by the production of a characteristic DNA fragment which results from enzyme cutting at A.

There is no simple closed solution to the coupled, nonlinear equations specified by eq 1. However, if the following specific experimental conditions can be shown to pertain, the kinetic expression which describes product formation simplifies greatly: (a) the underlying DNA conformational equilibrium is slow compared to the enzyme cutting rate, i.e.

$$k_3 >> k_1 + k_{-1}$$

(b) the enzyme has been administered at a high concentration, i.e.

$$E_0 A_0 k_2 >> k_1 + k_{-1}$$

This second criterion specifies that the enzyme binding reaction has been made faster than substrate isomerization.

These two boundary conditions predict that, upon mixing the enzyme and the DNA substrate, the rate of product formation will be biphasic. The fraction of DNA which exists in the enzyme-sensitive conformation at equilibrium (A_0/C_T) will be cut rapidly after addition of enzyme. After that rapid phase is complete, additional product (site-specific cuts at A) will be produced only after substrate isomerization has occurred. That second phase is limited by the rate of formation of the enzyme-sensitive conformation. Below we list the rate equation for such a simplified biphasic solution to the kinetic scheme

$$P/C_T = (A_0/C_T)[1 - \exp(-k_3 E_0 t)] + (1 - A_0/C_T)[1 - \exp(-k_1 t)] \qquad (2)$$

where P/C_T is the fraction of total DNA molecules cut specifically at the site of interest, A_0/C_T is the fraction of total molecules in the enzyme-sensitive state at $t = 0$, and $1 - A_0/C_T$ is the fraction of molecules in the enzyme-insensitive conformation at $t = 0$. We define an equilibrium constant

$$K = A_0/B_0 = k_1/k_{-1}$$

and take advantage of the identities:

$$C_T = A_0 + B_0$$

$$B_0/C_T = 1/(1 + K)$$

Equation 2 implies that if experiments are considered where the fraction of cut molecules remains small, the second exponential term in eq 2 will linearize. Since the initial bimolecular cutting process is fast (by definition), the measurable S1 cutting kinetics at A will converge to a linear time dependence.

The slope of those linearized kinetics is directly related to the rate of formation of the S1-sensitive conformer:

$$\frac{\partial(P/C_T)}{\partial t} \cong (1 - A_0/C_T)k_1 = k_1/(1 + K) \qquad (3)$$

while extrapolation of the linearized data to $t = 0$ is a measure of the equilibrium constant for formation of the enzyme-sensitive conformer

$$\lim_{t \to 0} P/C_T \cong A_0/C_T = \frac{1}{1/K + 1} \qquad (4)$$

Results

Kinetic Analysis of pM-HX. We have initiated our studies using the plasmid pM-HX. This plasmid contains a 3.5 kb *Hin*dIII–*Xba*I fragment of human DNA inserted into the corresponding sites of pUC12. This insert carries the entire first exon of the human c-*myc* gene along with about 2 kb of 5′-flanking sequence (see Figure 1C for a schematic representation of the plasmid).

To assay for the presence of alternative (S1-sensitive) DNA secondary structure in pM-HX, we digest supercoiled plasmid with S1 nuclease, purify the DNA by phenol extraction and

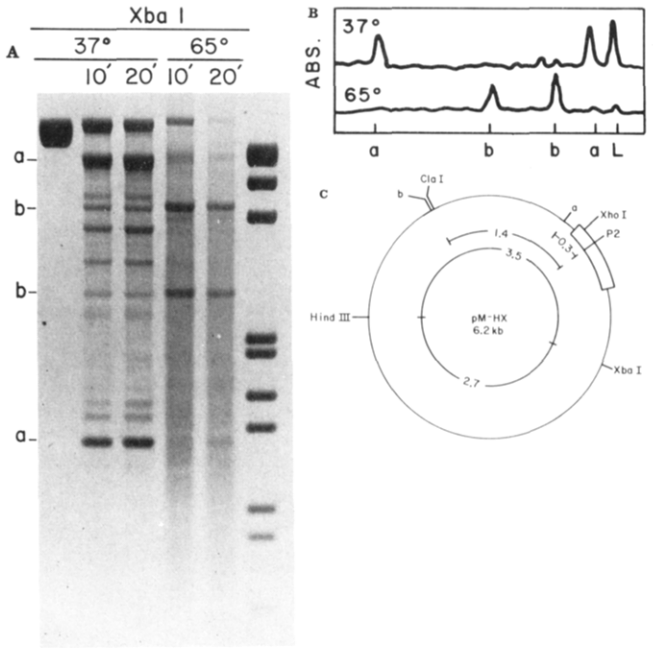

FIGURE 1: Low-resolution mapping of S1-sensitive sites in the human c-*myc* gene. (A) Supercoiled pM-HX DNA was isolated from *E. coli* HB101. DNA was dissolved in S1 digestion buffer and incubated at either 37 or 65 °C for 15 min. After being cooled to 37 °C, the samples were digested with S1 nuclease (250 units of S1/μg of DNA, 100 μg/mL DNA) for 10 or 20 min. Control samples were incubated without S1 for 20 min. DNA was purified by phenol extraction and ethanol precipitation and restricted with *Xba*I. DNA samples were electrophoresed in TAE (40 mM Tris–acetate, 5 mM sodium acetate, and 2 mM EDTA), 1.4% agarose gels. A negative image of the ethidium bromide stained gel is shown. The bands which define the major S1 cleavage sites in c-*myc* are marked a and b. The markers are *Eco*RI–*Hin*dIII-digested λ DNA. (B) The trace corresponds to optical densitometry of data measured after 10-min incubation with S1. (C) Schematic diagram of pM-HX. The S1-sensitive sites a and b are indicated along with their distance (in kilobase pairs) from the major promoter site P2 (Battey et al., 1983). Also shown are the positions of relevant restriction sites. The thickened portion of the line represents the first exon of the c-*myc* gene. The orientation of the *myc* sequence, 5′ to 3′, is clockwise.

ethanol precipitation, and then cleave with a restriction enzyme which has a single recognition site in the plasmid. The samples are electrophoresed in an agarose gel under native conditions, and the digestion products are visualized by ethidium bromide staining. In this assay, site-specific double-strand S1 cleavage is indicated by a pair of discrete subbands, whose combined length equals the length of the plasmid. The position of S1-sensitive sites is determined by comparing the size of the fragments produced in experiments using different restriction enzymes for secondary cleavage.

We have identified two DNA segments within the 5′-flanking region of the gene which are capable of assuming an S1-sensitive secondary structure. The analyses are displayed in Figure 1A, and a low-resolution map of those enzyme cutting sites is illustrated in Figure 1C. Site a maps to a region approximately −270 base pairs (bp) from the most commonly used cap site P2 (Battey et al., 1983). Under standard conditions of analysis (Figure 1A), nearly 40% of plasmid molecules have been cut specifically at site a. That quantity will be analyzed below in terms of a detailed kinetic formalism. S1 nuclease cutting at site b occurs at −1400 bp relative to P2. The conformational equilibrium responsible for S1 cutting at site b is interesting in that it is very temperature sensitive. As seen in Figure 1A, when pM-HX is incubated briefly at 65 °C and then cooled to 37 °C prior to S1 nuclease cutting, the plasmid substrate undergoes a slowly reversible, conformational change; i.e., an S1-sensitive conformation at site b becomes very favorable (greater than 50% of plasmid molecules are cut specifically at site b under standard conditions). Moreover, that conformational change is accompanied by a significant destabilization of the S1-sensitive conformation at site a (specific S1 cutting at site a disappears upon formation of an S1 cutting site at site b).

As seen in Figure 3 and below, the conformational equilibria which give rise to site specific cutting at site a or site b are driven by supercoiling of the DNA substrate. Because of that coupling, these equilibria necessarily compete with one another for the available supercoil energy. Cantor and colleagues have described such behavior within the 5′ end of the chicken globin gene (Cantor et al., 1984). We suggest that the human c-*myc* gene displays a similar type of coupled, competitive equilibrium within its 5′-flanking regions. The potential biological significance of such long-distance structural effects will be discussed below.

We note the presence of secondary cutting sites in the plasmid pM-HX, especially obvious in highly supercoiled substrates (Figures 1A and 3). These sites map to sequences in the pUC12 vector (data not shown) and are not detected in plasmids with lower superhelical density (Figure 3). For that reason, we have not explored those structure features in detail.

We have mapped c-*myc* sites a and b at high resolution. S1 digestion was performed as in Figure 1. S1-digested material was then phosphatased and 5′ end labeled with [γ-^{32}P]ATP and polynucleotide kinase to label the S1-generated ends. The labeled DNA was subsequently restricted with an enzyme which cleaves within 200 bp of the S1 cleavage sites (see Figure 1C, *Xho*I for site a and *Cla*I for site b). The restriction cleavage was chosen so that the S1-linearized plasmids are split into two fragments, only one of which will be small enough to enter a sequencing gel. Lengths have been determined relative to the product of standard Maxam–Gilbert chemical strand break chemistry.

Figure 2 shows the results of the high-resolution mapping. The a site is located in a region of tandem repeats of the sequence 5′-CCCTCCCC-3′ which lies from −315 to −262 bp relative to the P2 transcription origin. The most intense cutting is at a 2-base-long site at the 3′ end of the cluster, although secondary cutting sites can be seen in the other repeat elements upon substantial overexposure.

Site b occurs at the 5′ end of a long polypyrimidine segment (Figure 2B) which extends from −1437 to −1421 bp relative to the P2 transcription origin. Interestingly, a 15 bp polypyrimidine segment located 17 bp upstream from site b is not cut by S1 (see upper portion of Figure 2B). We caution that since we are using moderately high S1 concentration, the ends of the molecules may have undergone some exonucleolytic nibbling following linearization. Therefore, the positions of cleavage might not be the primary sites of S1 attack. However, we believe that substantial "nibbling" has not occurred, as indicated by the rather compact cleavage distributions.

We have chosen to concentrate our efforts on characterizing the properties of the a site. One reason for this is that it is located very near to sequences important for transcriptional regulation of the gene (Battey et al., 1983). Another reaon is that it is unusually stable under physiological conditions of supercoiling and temperature (see below). These properties make this site especially interesting, and at the same time make it easily accessible to study.

Figure 4 shows an experiment which follows the time course of S1 digestion at site a, at two different S1 concentrations.

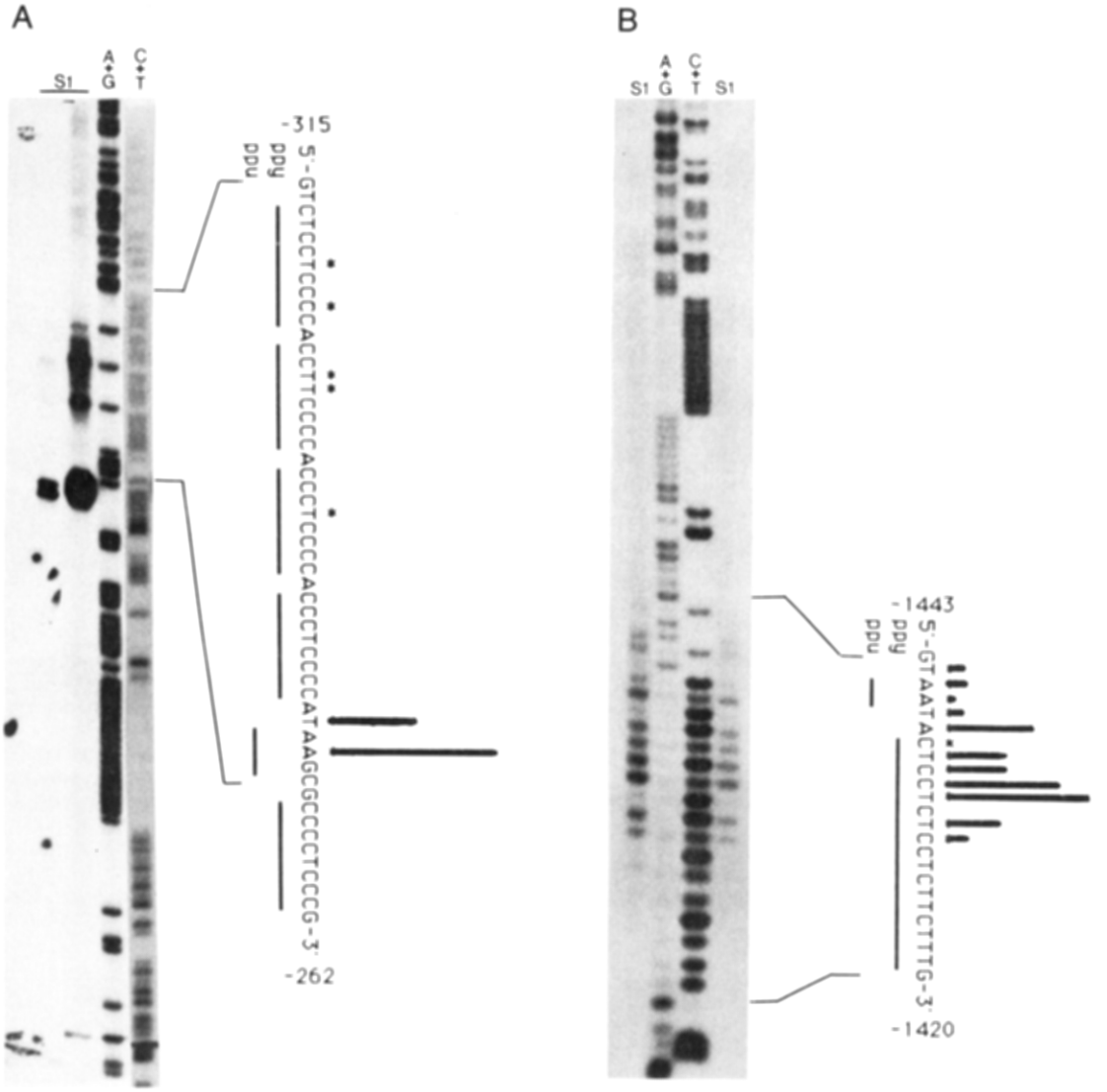

FIGURE 2: High-resolution mapping of S1-sensitive sites in pM-HX. (A) The a site: Highly supercoiled pM-HX DNA ($\sigma = -0.1$) was prepared by the ligase method as described under Materials and Methods. The DNA was digested with S1 nuclease as described in Figure 1. After phenol extraction and ethanol precipitation, the DNA was treated with calf alkaline phosphatase and 5′ end labeled with polynucleotide kinase and [γ-^{32}P]ATP as described (Maniatis et al., 1982). Labeled DNA was cleaved with *Xho*I and electrophoresed with markers in an 8% acrylamide–8 M urea sequencing gel (lanes marked S1). The left-most lane is an underexposure of the right. The markers are A + G and C + T sequencing ladders (Maxam & Gilbert, 1980) prepared from the 2 kb *Hin*dIII–*Xho*I fragment of pM-HX. Marker fragments were uniquely 3′ end labeled at the *Xho*I site with Klenow fragment and [γ-^{32}P]dNTP's as described (Maniatis et al., 1982). The 3′ end labeling reaction was carried out so that the 4-base recessed 3′ end of the *Xho*I site was completely filled in. Therefore, a marker DNA fragment will be 4 bases longer than an S1-generated fragment that has an identical 5′ terminus. The right side of the figure displays the DNA sequence in the region of S1 cleavage. Horizontal bars identify the position and relative likelihood of principle S1 cutting sites (measured by densitometry). The asterisks mark the positions of secondary S1 cleavage sites. Vertical bars indicate the position of polypurine tracks. (B) The b site: Analysis was performed as detailed above, with the exception that the DNA was heated at 65 °C for 15 min prior to S1 digestion at 37 °C, and secondary digestion was with *Cla*I instead of *Xho*I. Marker sequencing ladders were prepared from the 1 kb *Hin*dIII–*Cla*I fragment of pM-HX. Since *Cla*I creates 2-base recessed 3′ ends, marker fragments are 2 bases longer than S1-generated fragments with identical 5′ ends. All other symbols are as for site a.

As seen, doubling the enzyme concentration has no systematic effect on the kinetics of specific cleavage. From this rather unique enzyme concentration independence, we conclude that the rate of cutting at site a may be limited by a slow first-order equilibrium between an S1-sensitive and an S1-insensitive conformation, as described in the kinetic formalism under Materials and Methods.

Figure 3 displays S1 cutting kinetics at the a site as a function of superhelical density. Plasmids of defined superhelical density were prepared by relaxing samples with eukaryotic topoisomerase I in the presence of varying amounts of ethidium bromide (see Materials and Methods). The time course of S1 digestion at the a site was then measured at a high limiting S1 concentration. As seen, there appears to be a threshold value of supercoiling required for the formation of an S1-sensitive conformational isomer at site a. This threshold value occurs at moderate values, near the physiological range ($\sigma < -0.066$). At higher values of supercoiling (lower σ), the equilibrium is driven increasingly in favor of the S1-sensitive conformation.

We have quantitated these and similar kinetic data to show the fraction of plasmid specifically cleaved at site a for samples with differing superhelical density. These data are presented graphically in Figure 5. In all instances, cutting is linear with time and, where tested, is enzyme concentration independent. That enzyme concentration independence is an important piece of evidence which suggest that S1 cleavage rates have become limited by slow isomerization of the DNA substrate. As de-

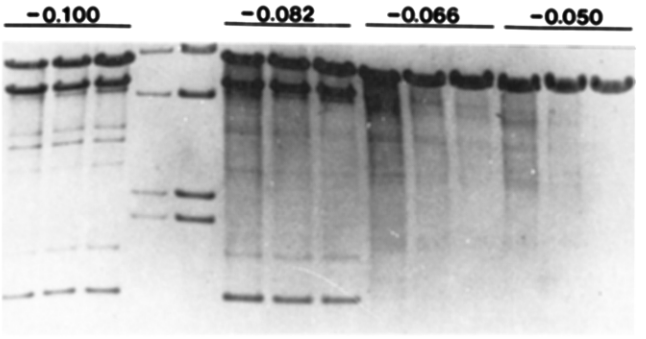

FIGURE 3: Response of S1 sites to superhelical density. Superhelical pM-HX was relaxed with eukaryotic topoisomerase I in the presence of varying amounts of ethidium bromide as described under Materials and Methods. Samples at the indicated superhelical density were digested with S1 nuclease at 37 °C for 10, 20, or 40 min (right to left). Secondary cleavage was performed with *Xba*I. The prominent subbands correspond to cleavage at the a site (~270 bp relative to the P2 promoter).

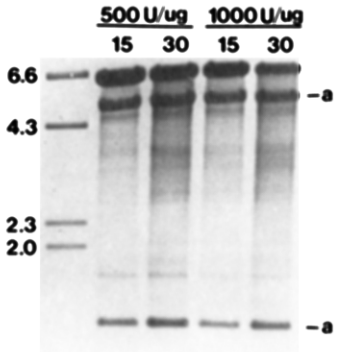

FIGURE 4: Dynamic behavior of the a site. Supercoiled pM-HX (isolated from HB101) was digested with the indicated dose of S1 nuclease (DNA concentration 100 μg/mL) for 15 or 30 min. After phenol extraction and ethanol precipitation, the samples were cleaved with *Xba*I. The markers were *Hin*dIII-cleaved λ. Notice the simple time dependence of S1 cleavage and that the kinetic data do not vary with enzyme concentration, as expected if cleavage has become limited by isomerization of the DNA substrate (see Materials and Methods).

rived under Materials and Methods, in the context of a two-state kinetic model for such substrate-limited kinetics, the slope of such a linear time course is determined largely by the rate constant for formation of the S1-sensitive isomer, and the intercept is determined by its equilibrium constant. The circles in Figure 5 correspond to data obtained from material with bacterial superhelical density (plasmids isolated from HB101, as in Figure 4). While we have not measured the superhelical density of this material directly, from literature values we believe it to lie in the range $-0.066 < \sigma < -0.075$ (Bauer, 1978). The triangles ($\sigma = -0.088$) and diamonds ($\sigma = -0.100$) correspond to cutting of plasmids supercoiled in vitro. These data have been fit to the kinetic formalism described under Material and Methods (eq 3), and the calculated kinetic parameters for the equilibrium are catalogued in Table I. As seen from Figure 5 and Table I, an extrapolation of the data to $t = 0$ (hence, the apparent equilibrium constant for formation of the S1-sensitive conformation) increases continuously with an increase of supercoil density. The increase in K_{eq} in going from native supercoil density to −0.088 is accompanied by an increase in the apparent opening rate constant (the slope of the kinetic curves). However, the increase in K_{eq} which occurs between −0.088 and −0.10 appears to be due to a closing rate change (the slope of the kinetic data does not change appreciably).

Kinetic Analysis of pHM3. We were interested in studying the conformational equilibrium at site a in a plasmid containing

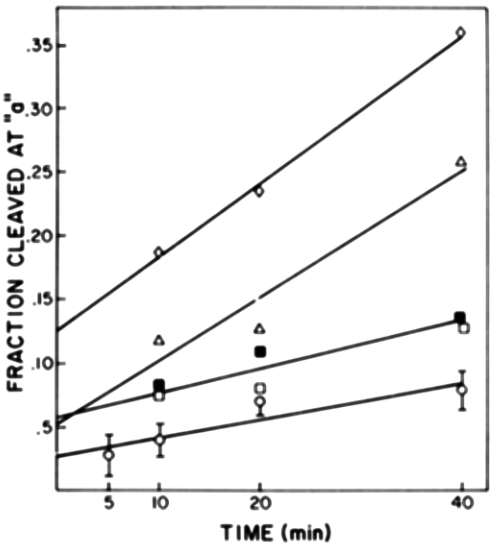

FIGURE 5: Kinetics of specific S1 cleavage at the a site in pM-HX. Supercoiled pM-HX (prepared from HB101, see Materials and Methods) was digested with S1 and secondarily cleaved with *Xba*I as in Figures 3 and 4. The extent of specific S1 cleavage at the a site was determined from densitometric scans of photographic negatives. (Circles) Cutting kinetics on plasmid pM-HX at (unaltered) physiological supercoil density. Error bars correspond to one standard deviation from the mean of three to six measurements. No systematic enzyme concentration dependence was detected above 500 units of S1/μg. Triangles are kinetics obtained from samples with a superhelical density of −0.088, while the diamonds were obtained from samples with a superhelical density of −0.100. (Squares) Supercoiled pM-HX (physiological supercoil density) was incubated with LMW factors obtained from 6B chromatography (5 OD units of LMW/OD unit of pM-HX) in S1 reaction buffer at 37 °C for 10 min. S1 nuclease was then added, and cutting kinetics were monitored: (closed squares) 500 units of S1/mg; (open squares) 1000 units of S1/μg of DNA.

Table I: Conformational Kinetics at Site a in pM-HX Calculated from a Two-State Model

physical state of plasmid DNA	K_{eq} ($\times 10^2$)[a]	k_1 ($\times 10^{-3}$ min^{-1})[b]	k_{-1} (min^{-1})[c]
native supercoil density (σ = −0.70)	2.7 ± 1.0	1.5 ± 0.4	5.5 ± 2.7
native supercoil density + pHM3 RNA	6.1 ± 0.2	2.0 ± 0.1	3.3 ± 0.2
supercoil density (σ = −0.088)	5.3 ± 3.8	5.2 ± 1.5	9.8 ± 7.9
supercoil density (σ = −0.10)	14 ± 1.0	6.6 ± 0.4	4.6 ± 0.5

[a] The equilibrium constant for formation of the S1 nuclease sensitive conformation at site a, calculated from linear regression of data in Figure 5, fit to eq 4 (see text). Error corresponds to one standard deviation from the calculated intercept. [b] The rate constant for formation of the S1-sensitive state, calculated from linear regression of data in Figure 5, in the context of eq 3 (see text). [c] The rate constant for dissipation of the S1-sensitive state, calculated by assuming $k_{-1} = k_1/K_{eq}$.

the entire c-*myc* sequence, pHM3 (see Materials and Methods and Figure 6B for a description of the plasmid). However, we were surprised to find that we could not observe S1 cleavage at the a site, even in plasmids at the maximum superhelical density attainable in vitro (see Figure 6). We observed secondary S1 cleavage sites elsewhere in the plasmid: at site e in the 3′-flanking region of the gene and at two other sites, c and d, which appear to map somewhere within the second exon. These secondary cleavage sites are mapped in Figure 6B. However, as can be deduced from Figure 6A, they appear only at the highest attainable supercoil denity and even then are unfavorable relative to the S1-insensitive conformer at those sites.

The data of Figure 3 show clearly that in the pM-HX subclone, the equilibrium which gives rise to an S1-sensitive

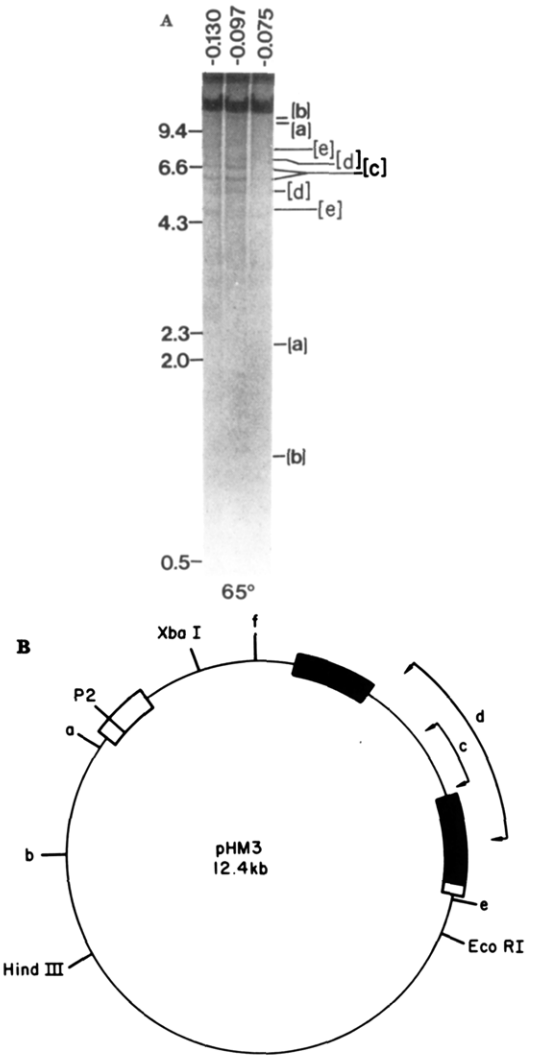

FIGURE 6: S1 digestion of pHM3. Closed circular pHM3 DNA (Sepharose 6B purified to remove low molecular weight contaminants) was relaxed with topoisomerase I in the presence of ethidium bromide. (A) Samples with the indicated superhelical density (−0.075 to −0.13) were digested with S1 nuclease (500 units/μg of DNA, DNA at 50 μg/mL, 20 min at 37 °C). Secondary cleavage was with *Hin*dIII. a and b indicate the expected positions of fragments derived from cleavage at the corresponding sites in pM-HX. (B) Schematic diagram of pHM3 showing the positions of sites c, d, and e. As we have not confirmed the positions of sites c and d using restriction enzymes other than *Hin*dIII, we indicate the two possible positions of each of these sites as a pair of arrows connected by a bracket. Also presented for comparison are the positions of S1 sites which we have identified in pM-HX (sites a and b) and a site we have identified in a subclone of the first exon (site f).

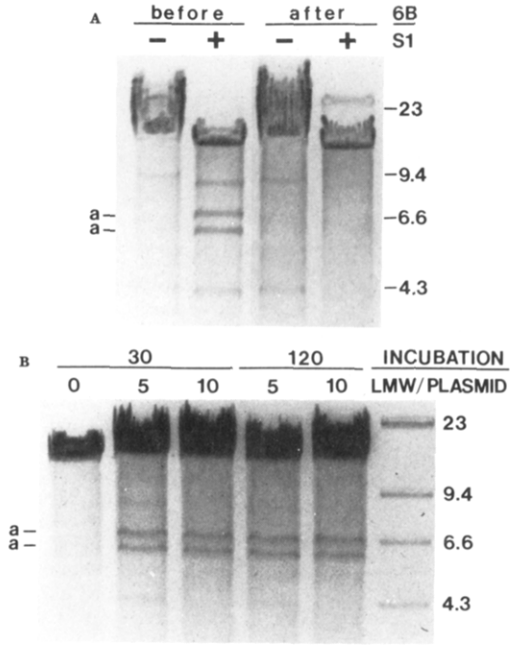

FIGURE 7: Conditions required for S1 digestion of the a site in pHM3. (A) S1 digestion of "crude" pHM3 preparations. Closed circular pHM3 DNA was purified by alkaline extraction and CsCl–ethidium bromide gradient centrifugation. 4-μg aliquots of plasmid were digested with S1 (+ lanes) before or after chromatography on Sepharose 6B as described under Materials and Methods. Secondary cleavage was with *Eco*RI. The (−) lanes are samples which were mock-digested without S1 nuclease. The prominent subbands in the "before, +" lane are due to cleavage at the a site. The faint subbands seen in all four lanes are due to a minor specificity of the *Eco*RI preparation used in these experiments. (B) Effect of low molecular weight factors on S1 cleavage of pHM3. CsCl gradient purified plasmid was subjected to Sepharose 6B chromatography, and material eluting in the included volume was deproteinized and then concentrated as described under Materials and Methods. The absorbance of the low molecular weight fraction (LMW) was determined at 260 nm. Low molecular weight material was added to 6B-purified pHM3 DNA at ratios of 0, 5, and 10 (OD LMW/OD plasmid). The mixtures were incubated in S1 buffer at 37 °C for 30 or 120 min and then digested with S1 nuclease (1000 units/μg of DNA, 20 min, 50 μg/mL DNA). Secondary cleavage was with *Eco*RI. Note that S1 cleavage at site a is fully regenerated in pHM3 at an added mass ratio of 5.

conformation at site a is driven by the free energy of supercoiling. Yet, when embedded in a larger fragment of the c-*myc* gene, the equilibrium which gives rise to S1 sensitivity at site a remains unfavorable at any achievable supercoil density, in spite of the fact that the DNA sequence in the two plasmids is identical for 1500 bases to either side of site a. We have shown that the full-length c-*myc* plasmid contains several sites within its 3′ end which can assume an altered S1-sensitive secondary structure upon supercoiling. The pM-HX subclone is derived by eliminating those 3′ segments. Therefore, as we have described for the 5′ end of the gene, we propose that the secondary structure equilibrium at site a may compete for the available supercoil energy with sites within the 3′ end of the gene.

As described under Materials and Methods, we routinely purify our plasmids by gel filtration (Sepharose 6B) after CsCl–ethidium bromide centrifugation. However, when that column purification step is omitted, we find that site a in the full-sized clone becomes quite sensitive to S1 digestion. This observation is reproduced in Figure 7A. CsCl-banded pHM3 was deproteinized and then divided into two samples. One sample was passed through a 6B column; the other sample was not. Both were digested with S1 under identical conditions, and a secondary digest was performed with *Eco*RI. Specific cleavage at the a site is expected to give rise to a pair subbands migrating at 5.8 and 6.6 kb. As seen in Figure 7A, S1 nuclease sensitivity at site a is lost after column purification. We have confirmed that 5′ cutting is occurring at site a by using a different restriction enzyme for secondary cleavage and have verified that the fractionation procedure does not introduce strand breaks in the plasmid (not shown).

These findings suggested to us that some low molecular weight factor present in deproteinized material is able to influence the structural equilibrium which occurs at the a site. To test this proposal, we ran a sample of CsCl-banded pHM3 through a Sepharose 6B column to purify the low molecular weight (LMW) UV-absorbing material which copurifies with the plasmid. We have determined that in standard preparations of pHM3, the ratio of LMW material to plasmid in the CsCl-banded material is about 5, as estimated by the UV

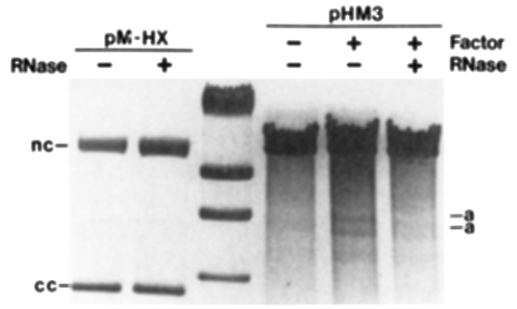

FIGURE 8: Sensitivity of low molecular weight factors to RNase. LMW factors were isolated as in Figure 7. An aliquot of the factors was digested with RNase T1 as described under Materials and Methods (factor +, RNase + lane). Another aliquot was mock-digested in parallel without T1 (factor +, RNase – lanes). After purification by phenol extraction and ethanol precipitation, RNase-treated and control factors were mixed with samples of 6B-purified pHM3 DNA in S1 buffer and incubated for 10 min at 37 °C. A third sample (factor –, RNase –) contained only 6B-purified pHM3. S1 nuclease (500 units/μg of DNA) was added, and the samples were digested for 20 min. The left-most lanes correspond to an assay for DNase activity in the RNase preparations. A mixture of nicked (nc) and closed circular (cc) pM-HX was treated with RNase under conditions identical with those used for treatment the LMW factor. As seen, closed circular material does not appear to be nicked by the treatment (compare the + and – RNase lanes).

absorbance profiles of the column (data not shown). Aliquots of the isolated LMW material were exhaustively deproteinized with phenol and then were added back to 6B-purified pHM3 in S1 reaction buffer, 37 °C. The samples were then digested with S1 and restricted with *Eco*RI as in Figure 7A. The results are shown in Figure 7B. DNA samples incubated with deproteinized LMW material show S1-specific subbands of 6.6 and 5.7 kb, characteristic of cleavage at the a site. We have confirmed the position of cleavage with another restriction enzyme (data not shown).

We have subjected aliquots of the LMW material to various chemical and enzymatic treatments in an effort to determine the chemical identity of the component which induces the formation of an S1-sensitive conformation at site a. In an experiment shown in Figure 8, we digested LMW material with RNase T1 and then assayed its ability to restore S1 sensitivity at the a site of 6B-purified pHM3. As seen, RNase-treated LMW material was incapable of conferring S1 sensitivity. In other experiments (data not shown), we have demonstrated that the capacity to confer S1 sensitivity at site a is unaffected by pretreatment of LMW with DNaseI. We have also determined that the LMW material is inactivated by mild alkaline hydrolysis (0.3 N KOH, 8 h, 37 °C). Each of these experiments supports the conclusion that the active species in the LMW fraction is RNA.

RNA Binding to pM-HX. To elucidate the mechanism of this RNA-induced enhancement of S1 cutting at site a, we have studied the effects of pHM3 RNA on S1 digestion at the a site in the subclone pM-HX. Concentrated LMW factor was purified as above. An aliquot was then added to column-purified pM-HX DNA (bacterial superhelical density) in S1 buffer and incubated for 30 min at 37 °C. S1 was added at a limiting high concentration, and site-specific DNA cleavage at site a was monitored as a function of time. The fraction of plasmid specifically cleaved at the a site was then quantitated and has been plotted in Figure 5A (square symbols). At the LMW effector concentration employed (OD_{260} LMW/OD_{260} plasmid = 5), the LMW fraction increases S1 nuclease cutting at site a substantially. On the basis of the kinetic data (Figure 5, Table I), we conclude that LMW RNA has shifted the conformational equilibrium at site a by a factor of 2. However, the slope of the time course is unchanged, indicating that the RNA does not affect the apparent rate constant for formation of the S1-sensitive conformation. By inference, we conclude that (RNA within) the LMW fraction alters the conformational equilibrium at site a by slowing the rate of return (k_{-1}) to the S1-insensitive conformation (Table I). In principle, the effect upon S1 cutting could have been due to association with the enzyme itself. However, on the basis of the fact that the measured cutting rate and the specificity of enzyme cutting on pM-HX are unaffected by the LMW RNA, we feel that a direct affect due to RNA–enzyme binding is not compatible with the data.

We summarize our results in terms of a preliminary kinetic model for the effect of RNA on S1 digestion at site a in the c-*myc* gene. We propose that DNA at site a engages in a slow first-order equilibrium between an S1-sensitive and an S1-insensitive conformation. The equilibrium is driven in the direction of the S1-sensitive conformation by supercoiling (Figure 3). In the full-length genomic clone, the energy available to drive formation of an S1-sensitive conformation at site a is greatly reduced due to competition with equilibria at other nearby sites (Figure 6). As a result, the equilibrium at site a is sufficiently unfavorable in pHM3 that S1 cutting is undetectable in our assay at any achievable supercoil density (Figure 6). We propose that an RNA component of the LMW fraction can interact specifically with the S1-sensitive a conformer, thereby slowing its relaxation to the S1-insensitive conformation. This effect increases the equilibrium at site a to detectable levels in the genomic clone (Figures 7 and 8) and enhances the already favorable equilibrium at site a in the subcloned plasmid pM-HX (Figure 5, Table I).

Discussion

We have presented data which suggest that there are two well-defined segments of DNA within the 5′ end of the human c-*myc* gene (–270 and –1400 bp) which are adequately modeled as engaging in a slow equilibrium between a traditional helix structure and a stable, but atypical, structure which is identified by its sensitivity to S1 nuclease digestion in vitro.

Work is in progress to identify the structure of the S1-sensitive conformer at those two sites; however, at present, we would like to emphasize three aspects of these equilibria which are required by the kinetic data we have presented.

(a) The absolute stability of the alternative S1-sensitive conformer at either site is strongly dependent upon supercoiling of the DNA substrate (Figure 3). If DNA supercoiling is modulated in the nucleus, as suggested by others (Benyajati & Worcel, 1976), the secondary structure of DNA at the 5′ end of the c-*myc* gene may be sensitive to such modulation in vivo.

(b) At fixed supercoil density, the stability of the alternative conformer at site a is strongly dependent upon distant sequence effects. When placed nearby DNA corresponding to the 3′ end of the gene, the stability of the alternative helix conformation at site a is reduced significantly relative to its S1-insensitive conformer (Figure 6). Upon formation of an S1-sensitive conformation at –1400 bp, the S1-sensitive conformation at site a becomes very unfavorable and as a result is not detected by S1 analysis (Figure 1). We have ascribed such action at a distance to competition between distant conformational equilibria within the topologically constrained plasmid. Distant enhancers and/or repressor elements have been proposed to explain why expression of the c-*myc* gene appears to change as a function of its position in the genome (Lieder et al., 1983). In that regard, it is interesting to consider the possibility that in certain instances, such position effects

might be mediated by a DNA structural change of the kind we detect in cloned fragments of the gene.

(c) We have presented kinetic and structural data which suggest that RNA can interact specifically with the preexisting structural equilibrium at site a (Figure 5). The effect of this RNA species upon the kinetics of the equilibrium indicates that RNA behaves as a simple effector which drives the equilibrium by binding to and then trapping the S1-sensitive conformer at that site.

Clearly, the data at hand are insufficient to deduce the identity of the active RNA sequences within the preparations we have studied or to ascribe a functional significance to such RNA binding in a mammalian cell. However, we feel that it may be useful to outline two limiting classes of explanation for the RNA binding event, to serve as working hypotheses.

On the one hand, the interaction could be due to complementary base pairing between the RNA and a single-strand loop at the a site, thereby forming a D-loop structure. Such a proposal has precedence. Champoux and McConaughy (1975) have observed stable complexes between superhelical SV40 templates and transcription products synthesized in vitro by *E. coli* polymerase. Similarly, Radding and co-workers have demonstrated that homologous single-stranded DNA forms stable complexes with supercoiled plasmids by a D-loop mechanism (Holloman et al., 1975; Wiegland et al., 1977; Beattie et al., 1977). These D-loop structures are of sufficient stability to survive CsCl–ethidium bromide centrifugation (Wiegland et al., 1977). Since RNA–DNA hybrids are of greater stability than DNA–RNA duplexes, it seems likely that the complementary RNA would behave in a similar manner.

In the context of this limiting model, the underlying conformation equilibrium at site a must be the formation of a loop, presumably a bulge loop which results from slippage of the nine-nucleotide-long tandemly repeated sequence (−278 to −295 bp, see Figure 2). Single-strand loops of that kind would be greatly stabilized by Watson–Crick base pairing with a short, complementary RNA molecule and would be a highly preferred substrate for S1. However, it should be noted that S1 cutting at site a is not distributed over a loop-sized grouping of bases (Figure 2) but is instead localized to a discrete, two-base segment at the 3′ end of the tandem sequence repeat. We find it difficult to construct a loop model based upon slippage of the tandem sequence repeat at site a which is consistent with that detailed S1 cutting pattern. However, given the uncertain relation between secondary structure, enzyme binding, and enzyme cutting for S1, we cannot rule out a loop model based upon S1 cutting data at this time.

In an alternative model, we propose that RNA may bind to site a by formation of a triple-strand complex. Such structures have been observed in experiments with synthetic polynucleotides, the best studied example being poly(dT)–poly(dA)·poly(dT) (Arnott & Selsing, 1974). In such a triplex, an anti-parallel DNA or RNA duplex serves as a lattice around which a third DNA or RNA strand is wound. Pairing of the third strand is due to Hoogsteen or reversed-Hoogsteen pairing within the major groove of the core duplex. To accommodate a third DNA or RNA strand in the major groove, the core duplex must assume an A-type secondary structure (Arnott & Selsing, 1974). Consequently, for most DNA duplexes, it is likely that the binding event responsible for triple-strand formation will be accompanied by a B to A helix structure transition.

While there is no precedent for the formation of triple-strand helices with naturally occurring DNA sequences, the a site has characteristics expected for a duplex which could form a triplex; e.g., the site has polypurine–polypyrimidine symmetry and has substantial poly(dG)–poly(dC) character. Evidence from several sources suggests that such sequences tend to form an A or A-like helix geometry in solution (McCall et al., 1985; Drew & Travers, 1984).

In view of these arguments, we suggest a second working hypothesis to explain the effect of RNA binding at site a. We suggest that the conformation equilibrium which we have detected at site a is a B to A helix transition. When the polypurine segment is in the A conformation, A–B junctions will be present at either end. Molecular modeling has suggest that such junctions can have a distorted conformation (Selsing, 1979). In our case, we propose that the junction nearest to the gene is sufficiently distorted to be recognized as a substrate for S1 nuclease. We suggest that the RNA effector interacts with the polypurine segment in its A conformation to form a relatively stable triple-strand complex. This slows the relaxation of the sequence back to B form, thereby increasing the equilibrium constant for formation of the S1-sensitive state.

If the DNA structure equilibrium we have monitored at the 5′ end of the human c-*myc* gene has regulatory significance, cellular factors which stabilize the S1-sensitive conformer might serve as regulatory factors. Our results suggest that single-strand RNA could serve as such a trans-acting factor. This idea is reminiscent of the model for gene regulation put forth by Britten and Davidson (1969). At present, we are not aware of any systems which utilize regulatory RNA species of this kind; however, the concept may be worth consideration and is being tested in our laboratory.

References

Arnott, S., & Selsing, E. (1974) *J. Mol. Biol. 88*, 509–521.

Battey, J., Moulding, C., Taub, R., Murphy, W., Stewart, T., Potter, H., Lenoir, G., & Leder, P. (1983) *Cell (Cambridge, Mass.) 34*, 779–787.

Bauer, W. R. (1978) *Annu. Rev. Biophys. Bioeng. 7*, 287–313.

Bauer, W. R., & Vinograd, J. (1968) *J. Mol. Biol. 33*, 141–171.

Beattie, K. L., Wiegland, R. C., & Radding, C. M. (1977) *J. Mol. Biol. 116*, 783–803.

Benyajati, C., & Worcel, A. (1976) *Cell (Cambridge, Mass.) 9*, 393–407.

Bolivar, F., Rodriguez, R. L., Greene, P. J., Betlach, M. C., Heynecker, H. L., Boyer, H. B., Crosa, J. H., & Falkow, S. (1977) *Gene 2*, 95–113.

Britten, R. J., & Davidson, E. H. (1969) *Science (Washington, D.C.) 165*, 349–350.

Cantor, R. C., & Efstradiatis, A. (1984) *Nucleic Acids Res. 12*, 8059–8073.

Champoux, J. J., & McConaughy, B. L. (1975) *Biochemistry 14*, 307–316.

Drew, H. R., & Travers, A. A. (1984) *Cell (Cambridge, Mass.) 37*, 491–502.

Evans, T., Schon, E., Gora-Maslak, G., Patterson, J., & Efstradiatis, A. (1984) *Nucleic Acids Res. 12*, 8043–8059.

Hentschel, C. C. (1982) *Nature (London) 295*, 714–716.

Holloman, W. K., Wiegland, R., Hoessli, C., & Radding, C. M. (1975) *Proc. Natl. Acad. Sci. U.S.A. 72*, 2394–2398.

Klysik, J., Stirdivants, Larson, J. E., Hart, P. A., & Wells, R. D. (1981) *Nature (London) 290*, 671–677.

Kohwi-Shigematsu, T., & Kohwi, Y. (1985) *Cell (Cambridge, Mass.) 43*, 199–206.

Leder, P., Battey, J., Lenoir, G., Moulding, C., Murphy, W., Potter, H., Stewart, T., & Taub, R. (1983) *Science (Washington, D.C.) 222*, 765–771.

LePecq, J. B., & Paoletti, C. (1976) *J. Mol. Biol. 27*, 87-106.
Lilley, D. M. J. (1980) *Proc. Natl. Acad. Sci. U.S.A. 77*, 6468-6472.
Mace, H. A. F., Pelham, H. R. B., & Travers, A. A. (1983) *Nature (London) 304*, 555-557.
Maniatis, T., Fritsch, E. F., & Sambrook, J. (1982) *Molecular Cloning: A Laboratory Manual*, Cold Spring Harbor Laboratory, Cold Spring Harbor, NY.
Maxam, A., & Gilbert, W. (1980) *Methods Enzymol. 65*, 499-560.
McCall, M., Brown, T., & Kennard, O. (1985) *J. Mol. Biol. 183*, 385-396.
Messing, J. (1983) *Methods Enzymol. 101*, 20-78.
Mirkovitch, J., Mirault, M., & Laemmli, U. K. (1984) *Cell (Cambridge, Mass.) 39*, 223-232.
Nickol, J. M., & Felsenfeld, G. (1983) *Cell (Cambridge, Mass.) 35*, 467-477.
Paulson, J. R., & Laemmli, U. K. (1977) *Cell (Cambridge, Mass.) 12*, 817-828.
Pulleyblank, D. E., Haniford, D. B., & Morgan, A. R. (1985) *Cell (Cambridge, Mass.) 42*, 271-280.
Schon, E., Evans, T., Welsh, J., & Efstradiatis, A. (1983) *Cell (Cambridge, Mass.) 35*, 837-848.
Selsing, E., Well, R. D., Alden, C. J., & Arnott, S. (1979) *J. Biol. Chem. 254*, 5417-5422.
Siebenlist, U., Henninghausen, L., Battey, J., & Leder, P. (1984) *Cell (Cambridge, Mass.) 37*, 381-391.
Sinden, R. R., Carlson, J. O., & Pettijohn, D. E. (1980) *Cell (Cambridge, Mass.) 21*, 773-783.
Sinden, R. R., Broyles, S. S., & Pettijohn, D. E. (1983) *Proc. Natl. Acad. Sci. U.S.A. 80*, 1797-1801.
Viera, J., & Messing, J. (1982) *Gene 19*, 259-268.
Vinograd, J., Lebowitz, J., & Watson, R. (1968) *J. Mol. Biol. 33*, 173-180.
Wang, J. C., & Hogan, M. (1985) *J. Biol. Chem. 260*, 8194-8202.
Wiegland, R. C., Beattie, K. L., Holloman, W. K., & Radding, C. M. (1977) *J. Mol. Biol. 116*, 805-824.

Respective Role of Each of the Purine N7 Nitrogens of 5′-*O*-Triphosphoadenylyl(2′→5′)adenylyl(2′→5′)adenosine in Binding to and Activation of the RNase L of Mouse Cells

Jean-Claude Jamoulle,[‡] Krystyna Lesiak,[§] and Paul F. Torrence*

Laboratory of Chemistry, National Institute of Arthritis, Diabetes, and Digestive and Kidney Diseases, National Institutes of Health, Bethesda, Maryland 20892

Received April 25, 1986; Revised Manuscript Received August 6, 1986

ABSTRACT: Through a combination of chemical and enzymatic approaches a series of sequence-specific tubercidin-substituted ppp5′A2′p(5′A2′p)$_n$5′A (n = 1 to about 10; 2-5A) analogues were generated. In addition to the previously developed methodology of Imai and Torrence [Imai, J., & Torrence, P. F. (1985) *J. Org. Chem. 50*, 1418-1420], a new approach to synthesis of 2′,5′-linked oligonucleotides utilized adenosine in 3′,5′ linkage as a precursor to the targeted 5′-terminus of the desired product. For instance, A3′p5′A could be condensed under conditions of lead ion catalysis with tubercidin 5′-phosphate to give A3′p5′A2′p5′(c^{7}A). Treatment with the 3′,5′-specific nuclease P_1 led to p5′A2′p5′(c^{7}A). The combined use of the above procedures led to the synthesis of p5′(c^{7}A)2′p5′A2′p5′A, p5′A2′p5′(c^{7}A)2′p5′A, p5′A2′p5′A2′p5′(c^{7}A), and p5′A2p5′(c^{7}A)2′p5′(c^{7}A), which were converted to their corresponding 5′-triphosphates by the usual methods. Evaluation of these analogues for their ability to bind to and activate the 2-5A-dependent endonuclease (RNase L) of mouse L cells showed that there were small changes (≤10-fold) in the ability of the four tubercidin analogues to bind to RNase L. However, whenever the first and/or third adenosine nucleotide units were replaced by tubercidin, a dramatic decrease in ability to activate RNase L occurred. Only the second (from the 5′-terminus) adenosine residue could be replaced by tubercidin without any effect on RNase L activation ability.

2-5A[1] is a naturally occurring 2′,5′-linked oligonucleotide (Kerr & Brown, 1978) that is almost certainly involved in some of the antiviral effects of interferon [reviewed by Johnston and Torrence (1984)]. For instance, large amounts of 2-5A accumulate in interferon-treated encephalomyocarditis virus infected cells resulting in degradation of rRNA as well as poly(A+) RNA (Williams et al., 1979; Golgher et al., 1980; Knight et al., 1980). The complete 2-5A system currently includes the enzyme responsible for 2-5A generation or the 2-5A synthetase, the enzyme responsible for 2-5A action or the 2-5A-dependent endonuclease also known as RNase L, and a 2′,5′-phosphodiesterase that degrades 2-5A [reviewed by Johnston and Torrence (1984)]. The 2-5A system may also be involved in cell regulation and/or differentiation. For

[‡] Present address: Centre International de Recherches, Dermatologiques, Sophia Antipolis, Valbonne 06656, France.
[§] Present address: Center for Biomedical Research, University of Kansas, Lawrence, KS 66045.

[1] Abbreviations: 2-5A, ppp5′A2′p(5′A2′p)$_n$5′A, where n = 1 to about 10; 2-5A synthetase, the enzyme that, after activation by double-stranded RNA, effects the conversion nATP → pppA(pA)$_{n-1}$ + (n - 1)PP$_i$; PEI, poly(ethylenimine); HPLC, high-performance liquid chromatography; DMF, dimethylformamide; Tris-HCl, tris(hydroxymethyl)aminomethane hydrochloride.